Journal of Applied Physics ARTICLE scitation.org/journal/jap

Effect of carbon, oxygen, and intrinsic defects on hydrogen-related donor concentration in proton irradiated *n*-type silicon

Cite as: J. Appl. Phys. **130**, 115704 (2021); doi: 10.1063/5.0055769
Submitted: 3 May 2021 · Accepted: 22 August 2021 ·
Published Online: 16 September 2021

View Online Export Citation CrossMark

Akira Kiyoi,[1,2,a)] Naoyuki Kawabata,[1] Katsumi Nakamura,[3] and Yasufumi Fujiwara[2]

AFFILIATIONS

[1]Advanced Technology R&D Center, Mitsubishi Electric Corporation, 8-1-1 Tukaguchi-Honmachi, Amagasaki, Hyogo 661-8661, Japan
[2]Division of Materials and Manufacturing Science, Graduate School of Engineering, Osaka University, 2-1 Yamadaoka, Suita, Osaka 565-0871, Japan
[3]Power Device Works, Mitsubishi Electric Corporation, 1-1-1 Imajuku-Higashi, Nishi-ku, Fukuoka 819-0192, Japan

[a)]**Author to whom correspondence should be addressed:** Kiyoi.Akira@ay.MitsubishiElectric.co.jp

ABSTRACT

We investigated the effect of the concentration of carbon, oxygen, and irradiation-induced intrinsic defects on hydrogen-related donor (HD) concentration. Several *n*-type silicon wafers having different carbon and oxygen concentrations were irradiated with 2 MeV protons, subsequently annealed at 300–400 °C, and analyzed by spreading resistance profiling. The HD concentration had no correlation with carbon and oxygen concentration. Additionally, the HD concentration showed a strong increasing linear dependence with proton-irradiation dose at 350 and 400 °C and a square root dependence at 300 °C. In the decay process of HD concentration at 400 °C, fast- and slow-decay components were observed regardless of wafer type. Our results show that the HD formation is based on the interactive process of irradiation-induced intrinsic defects and hydrogen, rather than hydrogen-catalyzed thermal double donor formation. Magnetic-field-applied Czochralski (m:Cz) wafers with 300 mm diameter, which are critical for the production scaling of power devices, have a relatively higher oxygen concentration than conventional floating-zone wafers. Our results further suggest that controlling the intrinsic defect formation, rather than oxygen impurity concentration, is more important in realizing designed doping profiles with high accuracy and reproducibility for next-generation power devices using large-diameter m:Cz wafers as a standard starting material.

Published under an exclusive license by AIP Publishing. https://doi.org/10.1063/5.0055769

I. INTRODUCTION

The use of magnetic-applied Czochralski (m:Cz) wafers as a standard starting material to fabricate power devices has increased significantly in recent years because of the limitations of the conventional floating-zone (FZ) method such as limited production capacity and difficulties in the production of large-diameter wafers. The main difference between m:Cz and FZ wafers is the concentration of impurities (i.e., carbon and oxygen),[1] which affects the electrical properties of semiconductor power devices such as insulated gate bipolar transistors (IGBTs). The demand for high-performance IGBTs requires a precise understanding of the influence of relevant impurities in silicon materials. The electrical properties of IGBTs are affected by the impurities only when they are irradiated with electrons, protons, and helium ions for life-time modification or fabrication of field-stop (FS) layers.[2–6] In the fabrication of FS layers,[4–6] proton irradiation and subsequent annealing at moderate temperatures (300–500 °C) are used to induce donor states to increase the carrier concentration within layers.

Proton irradiation-induced donors have been phenomenologically speculated to be defect complexes containing hydrogen and ascribed to the so-called hydrogen-related donors (HDs). Although several reports investigating the nature of HDs are available in the literature,[7–30] their atomic structure has not yet been identified. It is known that the core of HDs evolves from crystal damages. Therefore, the donor states have been observed in crystalline silicon irradiated by neutrons,[9] electrons,[10–12] helium,[13,14] and protons,[15–23]

Published under an exclusive license by AIP Publishing

when enough hydrogen was available to form HDs via the reaction between hydrogen and the irradiation-induced defects. Using infrared electronic absorption, the existence of a group of donor states with ionization energies in the range of 34–53 meV has been revealed.[9–12] Additionally, the incorporation of hydrogen in HDs has been shown on the basis of shifts of electronic absorption energy with deuterium isotope substitution.[9,11,26] Based on experimental results and *ab initio* Density Functional Theory (DFT) calculations, atomic structures of HDs have also been studied. It has been suggested that oxygen-related defects [vacancy-oxygen complex (VO)[10,12] and interstitial carbon-interstitial oxygen complex (C_iO_i)][24,29,30] are associated with the formation of HDs. Furthermore, HDs related to intrinsic defects (vacancy and interstitial silicon and its cluster) have been also reported.[8,15,19–22] Therefore, a definitive identification of the core of HDs remains necessary. Moreover, it is well known that the formation of thermal double donors (TDDs)[31–33] are catalyzed by hydrogen[34–39] and irradiation damages,[40,41] making the interpretation of donor formation kinetics more complex in the silicon crystals, in which hydrogen, point defects, and oxygen coexist substantially. The role of oxygen in HD formation has been reported by Ulyashin *et al.*[39]

Recently, Schulze *et al.*[4] investigated the effect of carbon and oxygen on the doping profiles of an FS layer-based power device fabricated by proton irradiation doping. They found that the integrated FS dose, which corresponds to the total HD concentration induced by proton irradiation and moderate annealing, depended slightly on both carbon and oxygen concentration, but the investigated range of impurity concentration was limited typically for m:Cz wafers. On the contrary, we have confirmed that a substantial formation of HDs occurs even in pure epitaxial (epi) silicon using proton irradiation doping.[23] The physical mechanisms leading to HD formation should be clarified from the viewpoint of power device development and progressing hydrogen-related silicon science. Better understanding of relevant defects associated with HDs and their interactions with impurities are essential to realize the designed doping profiles with high accuracy and reproducibility using different kinds of silicon wafers. However, to date, these factors have not yet been investigated systematically.

Herein, in order to clarify the relevant defect associated with the HD formation process, we systematically investigated the effect of carbon concentration, oxygen concentration, and proton-irradiation dose on HD concentration by comparing the doping profiles of different wafers and irradiation dose at 300–400 °C using a spreading resistance (SR) profiling technique. Additionally, to distinguish the formation of TDDs and HDs, prolonged annealing experiments were performed.

II. EXPERIMENT

We used (100)-oriented phosphorus-doped *n*-type silicon wafers with similar phosphorus concentrations but different carbon and oxygen concentrations. Carbon and oxygen concentration were measured using a secondary ion mass spectrometry (SIMS) apparatus (IMS-7f, CAMECA, France). Additionally, to measure carbon concentration at lower levels than the detection limit of SIMS (5×10^{14} cm^{-3}), chemically activated deep-level transient spectroscopy (DLTS)[42] was employed. This method determines carbon concentration indirectly, based on C–H defects[43] induced by acid treatment. Phosphorus concentration was estimated from the carrier concentration of the bulk, which was measured by the SR profiling method. The phosphorus, carbon, and oxygen concentrations of each wafer are summarized in Table I.

TABLE I. Sample ID, crystal growth, and concentration of impurities in wafers.

		Concentration of impurities (cm^{-3})		
ID	Crystal growth	Phosphorus	Carbon	Oxygen
A	Epitaxial	5.1×10^{13}	5.6×10^{13}	$<5.0 \times 10^{15}$
B	FZ	6.4×10^{13}	1.8×10^{14}	$<5.0 \times 10^{15}$
C	FZ	6.6×10^{13}	1.0×10^{15}	$<5.0 \times 10^{15}$
D	FZ	6.8×10^{13}	2.0×10^{15}	9.9×10^{15}
E	m:Cz	4.5×10^{13}	1.1×10^{15}	1.6×10^{17}
F	m:Cz	5.3×10^{13}	5.1×10^{14}	1.6×10^{17}
G	m:Cz	7.9×10^{13}	5.0×10^{14}	1.4×10^{17}
H	m:Cz	7.2×10^{13}	3.6×10^{14}	1.6×10^{17}
I	m:Cz	6.3×10^{13}	1.3×10^{14}	1.7×10^{17}
J	m:Cz	5.5×10^{13}	1.1×10^{14}	1.8×10^{17}

The wafers were irradiated with 2 MeV protons using a cyclotron particle accelerator (CYPRIS-370 V, Sumitomo Heavy Industry, Ltd., Japan). The energy variation of the proton was 1.9 ± 0.1 eV. At this acceleration energy, according to SRIM2013 simulation program,[44] applying detailed calculations with full damage cascades, the depth of the projected ion range (R_p) was calculated to be 44.5 μm from the incident surface. The irradiation was performed intermittently at a sufficiently low beam current to avoid unintentional annealing during irradiation. The irradiation dose was in the range of 1×10^{12}–5×10^{14} cm^{-2}. This procedure guaranteed sample temperatures of <150 °C. After irradiation, the wafers were cut into a suitable size ($5 \times 5 \times 0.73$ mm^3) and annealed at temperatures of 300, 350, and 400 °C for 1 and 137 h in an oven under atmospheric air. The annealing temperature was controlled using a digital temperature controller equipped with a thermocouple placed close to the samples. After annealing, the samples were removed from the oven and immediately immersed in water to bring them to room temperature (approximately 25 °C). The samples were measured and analyzed by two-point SR profiling at approximately 25 °C with an SR profiler (SSM-2000, Solid State Measurements, Inc., USA) with a bevel angle of 2.5° to achieve an adequate depth resolution of 0.25 μm. The measured SR profiles were transformed into equivalent carrier concentration profiles via calibration with a standard (100)-silicon wafer, assuming that all regions exhibited *n*-type conductivity.

III. RESULTS

A. Effect of carbon and oxygen on HD formation

To investigate the role of carbon and oxygen in the formation of HDs, we compared the SR profiles of silicon wafers with different carbon and oxygen concentrations, irradiated with 2 MeV protons, and subsequently annealed at 300 °C for 1 h. Figure 1 shows the carrier concentration profiles of epi, FZ, and m:Cz

Published under an exclusive license by AIP Publishing

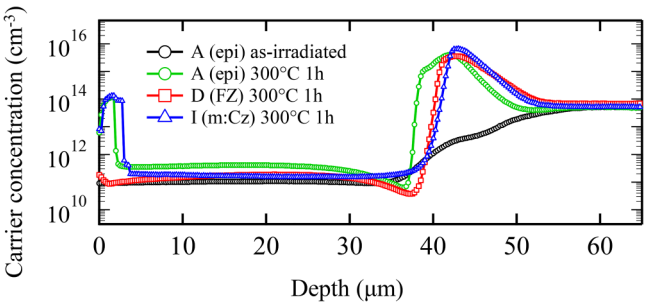

FIG. 1. Carrier concentration profiles of samples A (epi), D (FZ), and I (m:Cz) irradiated with 2 MeV protons at a dose of 3×10^{14} cm^{-2} and subsequently annealed at 300 °C for 1 h. The irradiated epi sample was also included for reference.

samples. The carrier concentration profile of the irradiated epi sample is also shown in Fig. 1. The profiles of hydrogen and the primary damage concentration, calculated with SRIM2013,[44] are shown to indicate the initial hydrogen and defect distribution of the wafers, respectively (Fig. 2). Calculated primary damage corresponds to vacancy concentration, but the same number of interstitial silicon is simultaneously created by irradiation.

Before annealing, a carrier compensation effect induced by radiation-induced shallow acceptor defects led to the reduction of carrier concentration across the proton penetrated layer. In contrast to Fig. 2, in Fig. 1, the carrier compensation effect was observed even beyond the penetration depth of the proton presumably because of the diffusion of the shallow acceptor defects. The shallow acceptor defect might be related to the hydrogenated multivacancy defect (V_2–H_2), which is demonstrated by the *ab initio* calculations presented by Coutinho *et al.*[45] After annealing at 300 °C, broad peaks of carrier concentration appeared around R_p (44.5 μm). These peaks correspond to the *n*-type region where the shallow HDs were induced due to the reaction between implanted hydrogen and radiation-induced defects on the diffusion pathway of hydrogen through the penetrated layer. We focused on these broad peaks in examining the nature of proton irradiation-induced

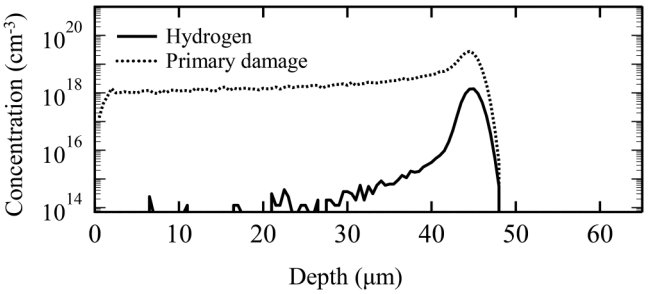

FIG. 2. Simulated hydrogen and primary damage profiles of silicon irradiated with 2 MeV protons at a dose of 3×10^{14} cm^{-2}. SRIM2013[44] was employed for this simulation.

HDs. Additionally, another shallow donor defect formation was observed near the surface. The profiles observed here were characteristic of proton irradiation doping processes.[4–6]

The peak carrier concentrations for samples A (epi), D (FZ), and I (m:Cz) were 4.0×10^{15}, 3.6×10^{15}, and 6.5×10^{15} cm^{-3}, respectively. We also measured the SR profiles of same wafer samples annealed at 350 and 400 °C because HDs occurring at different temperatures (250–600 °C) have been reported in the literature.[12,16] The peaks became broader as the annealing temperature increased due to the diffusion of implanted hydrogen, followed by the formation of HDs; nevertheless, the peak carrier concentrations were found to be comparable regardless of the wafer type at elevated temperatures (Fig. 3).

The correlation between HD and carbon and oxygen concentration is shown in Figs. 4 and 5, respectively. We evaluated a maximum and an integrated concentration of HDs at each annealing temperature. The maximum concentration of HDs was considered as the value of the peak near R_p, and the integrated concentration was calculated as the sum of the carrier concentration in the depth direction of the wafer, across the region where observed carrier concentration exceeds the original bulk carrier concentration of each wafer. In proton irradiation doping, carrier concentration depends on the substrate dopant (phosphorus in our samples) and the irradiation-induced dopant (i.e., shallow acceptor defect and HD). Accordingly, a calibration procedure was performed to extract the net HD concentration as follows: the concentration of HDs was estimated as the carrier concentration of annealed samples minus that of the corresponding irradiated samples, in which HDs were not formed based on the model described by Laven *et al.*[16] As shown in Fig. 4(a), the HD concentration remained practically constant at carbon concentration ranging from 5.6×10^{13} to 2.0×10^{15} cm^{-3} regardless of annealing temperature. For the epi sample annealed at 350 °C, the HD

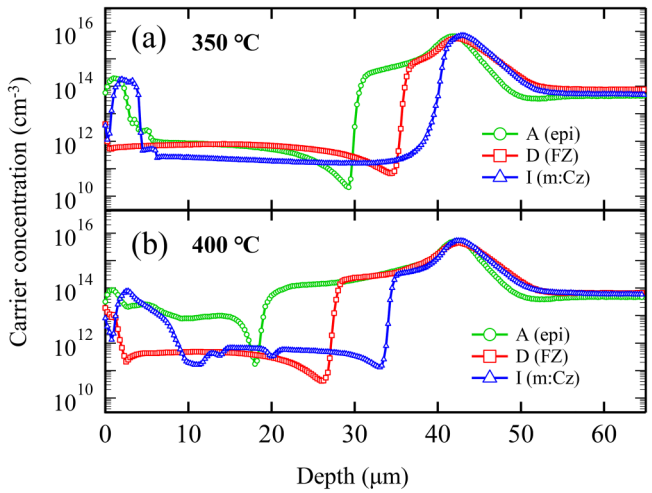

FIG. 3. Carrier concentration profiles of samples A (epi), D (FZ), and I (m:Cz) irradiated with 2 MeV protons with a dose of 3×10^{14} cm^{-2} and subsequently annealed at 350 and 400 °C for 1 h.

Published under an exclusive license by AIP Publishing

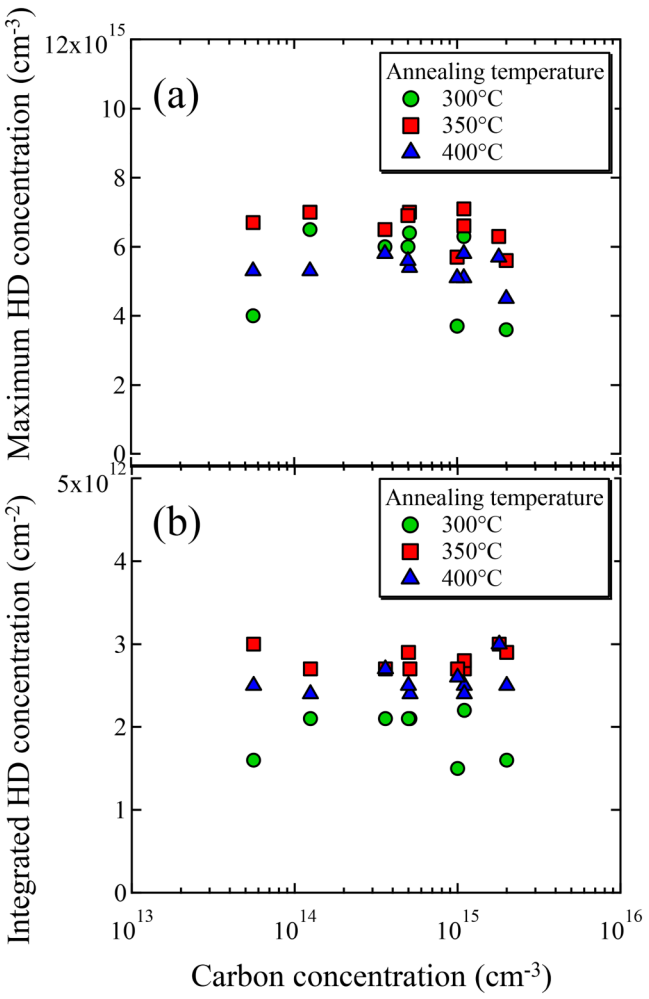

FIG. 4. Correlation between the hydrogen-related donor (HD) and carbon concentration for different wafers. (a) and (b) denote maximum and integrated HD concentration defined in the text, respectively. Circles, squares, and triangles correspond to samples annealed at 300, 350, and 400 °C for 1 h, respectively.

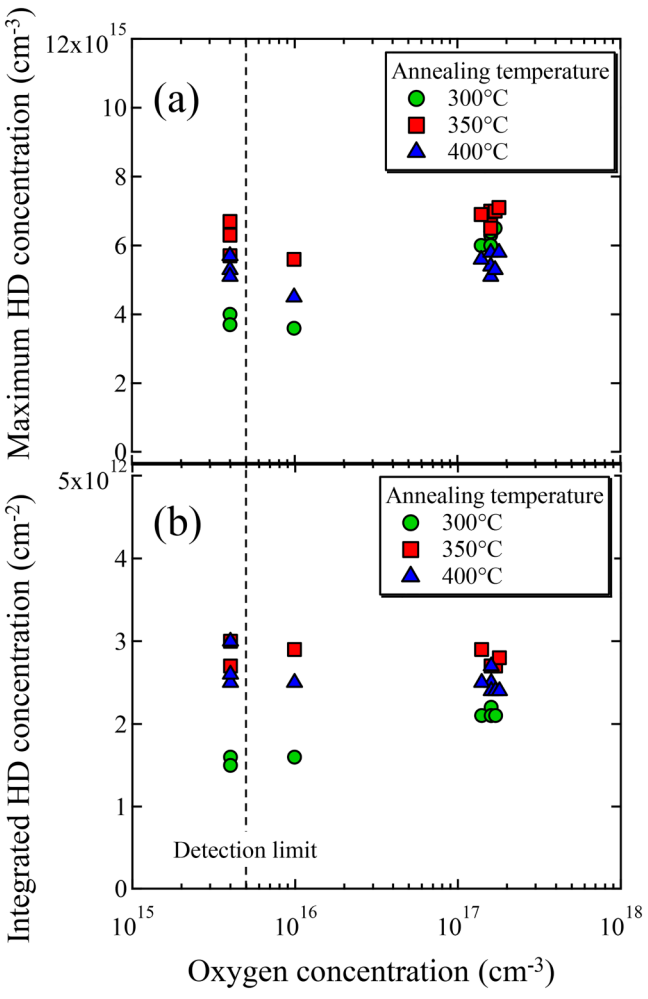

FIG. 5. Correlations between the hydrogen-related donor (HD) and oxygen concentration for different wafers. (a) and (b) denote maximum and integrated HD concentration defined in the text, respectively. Circles, squares, and triangles correspond to samples annealed at 300, 350, and 400 °C for 1 h, respectively. The detection limit of SIMS is shown as a dotted vertical line. The data points with oxygen concentration below the detection limit are placed at 4×10^{15} cm^{-3}.

concentration increased up to 7×10^{15} cm^{-3}, which exceeds the carbon concentration in the corresponding wafer by a factor of 100. The HD concentration also had no correlation with oxygen concentration in the range of less than 5×10^{15}–1.8×10^{17} cm^{-3}, as shown in Fig. 5. For oxygen-lean (<5×10^{15} cm^{-3}) wafers annealed at 350 and 400 °C, the HD concentrations were higher than the corresponding oxygen concentrations, as shown in Fig. 5(a). These results ruled out the direct incorporation of carbon and oxygen in the core of HDs.

The highest concentration of HDs was observed when samples were annealed at 350 °C, leading to the highest *n*-type doping activation factor, which is desired in the fabrication process of power devices. The authors hypothesize that this temperature behavior is due to a balance between the formation and partial dissociation of HDs at the studied temperature range (300–400 °C). It is assumed that the partial dissociation was induced by either the dissociation of HDs or the passivation of dangling bonds of defects[46] consisting of HDs, in which the passivation led to the deactivation of the shallow donor levels of HDs.

B. Effect of proton-irradiation dose on HD concentration

To investigate the correlation between the concentration of HDs and the intrinsic point defects induced by irradiation, we measured the SR profiles of the epi samples subjected to different proton-irradiation doses. Figure 6 shows the carrier concentration

Published under an exclusive license by AIP Publishing

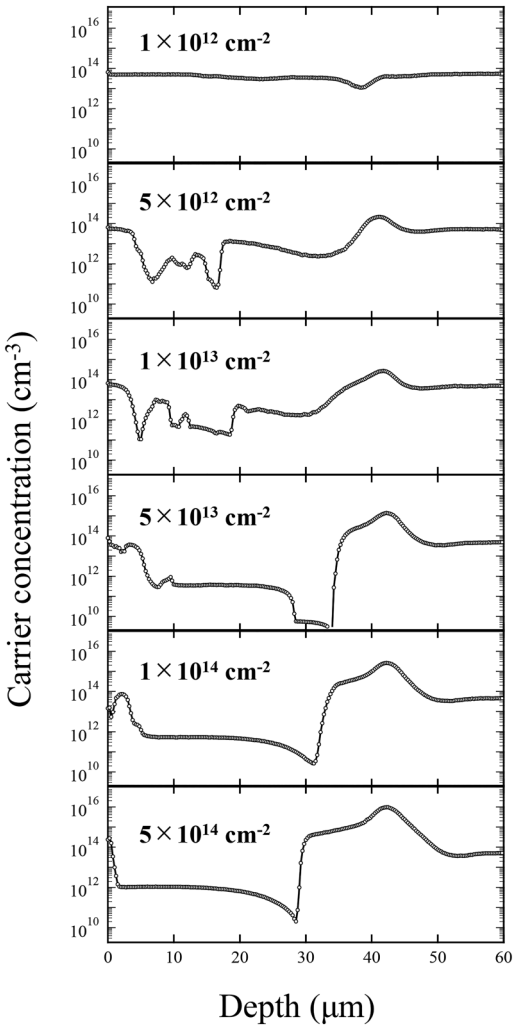

FIG. 6. Carrier concentration profiles of sample A(epi) after the irradiation of 2 MeV protons with doses varying from 1×10^{12} cm^{-2} to 5×10^{14} cm^{-2} and annealing at 350 °C for 1 h.

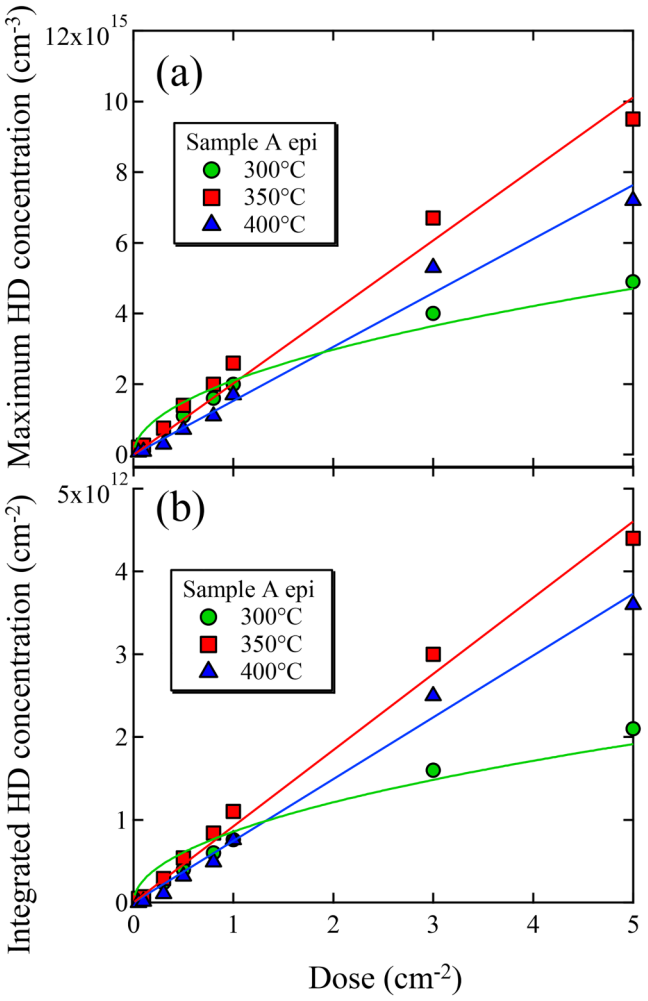

FIG. 7. Proton-irradiation dose dependence of the HD concentration for sample A (epi). (a) and (b) denote maximum and integrated HD concentration defined in the text, respectively. Circles, squares, and triangles correspond to samples annealed at 300, 350, and 400 °C, respectively.

profiles of epi samples irradiated with doses varying from 1×10^{12} to 5×10^{14} cm^{-2} and subsequently annealed at 350 °C for 1 h. The formation of HDs occurred near the R_p for all doses, except for the lowest dose (1×10^{12} cm^{-2}). Peak carrier concentrations increased monotonically with the increasing proton-irradiation dose. As shown in Fig. 7, the maximum and integrated HD concentrations showed an increasing square root dependence as the proton-irradiation dose increased at 300 °C, and a linear increasing dependence was observed at 350 and 400 °C. Job *et al.*[15] previously reported a similar linear dependence for proton irradiated *n*-type FZ silicon annealed at 370 °C. Different functional dependences may indicate the existence of different types of HDs evolving at different temperatures. The linear or square root dependence indicates the clear incorporation of intrinsic defects, such as vacancy, interstitial silicon, and its cluster, in the core of HDs.

Simulation results showed primary defects and hydrogen concentrations of 8×10^{15} and 4×10^{15} cm^{-3} at R_p, even at the lowest dose, assuming a scaling factor of 0.1 for the high recombination probability of induced primary defects.[47] This primary defect concentration is enough to create the HDs and support the direct incorporation of intrinsic defects in the HDs observed in this study. The saturation tendency of the HD concentration at 300 °C was observed at proton-irradiation doses of $>1 \times 10^{14}$ cm^{-2}, presumably due to over-passivation or the excessive condensation of intrinsic defects, leading to the inactivation of the donor nature of HDs.

Published under an exclusive license by AIP Publishing

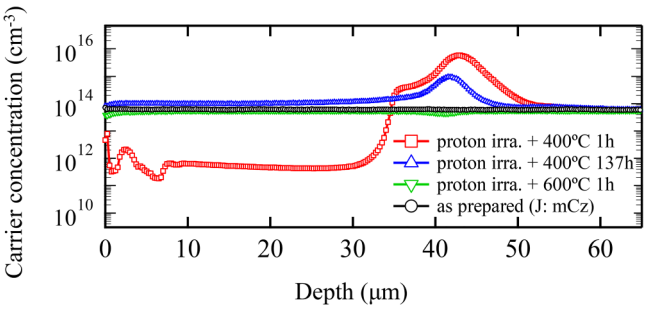

FIG. 8. Carrier concentration profiles of sample J (m:Cz) irradiated with 2 MeV protons with a dose of 3×10^{14} cm^{-2} and subsequently annealed at 400 °C for 1 and 137 h and at 600 °C for 1 h. The profile of m:Cz without irradiation and annealing is also displayed in the figure.

C. Thermal double donor

It is well known that hydrogen accelerates interstitial oxygen diffusion,[36,37] resulting in faster TDD formation.[34–39] The catalytic threshold of hydrogen concentration is estimated as 4.5×10^{10} cm^{-3} at 300 °C according to Ref. 38 and is much lower than the available hydrogen in proton-irradiated silicon wafers. Therefore, the hydrogen-catalyzed TDD and HD formation were assumed to contribute simultaneously to doping profiles in m:Cz wafers. To distinguish the contribution of HDs and TDDs to observed donor concentrations, we performed prolonged annealing for m:Cz samples because HDs are more thermally unstable than TDDs.[12,16]

Figure 8 shows the carrier concentration profiles of m:Cz samples annealed at 400 and 600 °C. The carrier concentration decreased from 5.8×10^{15} to 9.3×10^{14} cm^{-3} as annealing time increased from 1 to 137 h at 400 °C. Additionally, after annealing at 600 °C for 1 h, the carrier concentration profile completely recovered to that of the original wafer that did not receive proton irradiation (Fig. 8).

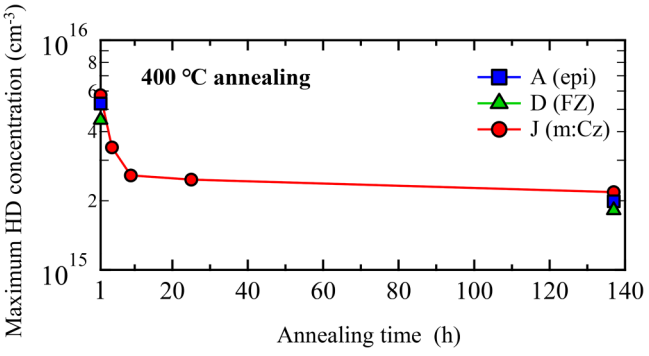

FIG. 9. Decay curve of the maximum HD concentration as a function of annealing time. The maximum HD concentration was estimated from sets of SR profiles of samples A (epi), D (FZ), and J (m:Cz) irradiated with 2 MeV protons with a dose of 3×10^{14} cm^{-2} and subsequently annealed at 400 °C.

Figure 9 shows the decay of the maximum HD concentration of the epi, FZ, and m:Cz samples as a function of annealing time at 400 °C. In the m:Cz sample, a fast decay was observed only at the initial stage of annealing, but donors still remained at the end of annealing even when the annealing time was prolonged up to 137 h. This result indicated the existence of at least two types of donors having different thermal stabilities. The contribution of the fast- and slow-decay donor components to total donor concentration for all wafer types was approximately 40% and 60%, respectively. The concentrations of fast- and slow-decay donor components were comparable among the silicon wafers. If the observed donor corresponded to TDDs, the donor concentration should have shown a dependence on oxygen concentration in the silicon wafers. This is because it is well known that the formation rate of TDDs strongly depends on oxygen concentration in silicon wafers.[31–33] Therefore, it is reasonable to assume that these donors correspond to HDs rather than TDDs. The fast-decay component of HDs dissociated at approximately 400 °C and the slow-decay component of HDs was stable up to approximately 500 °C. We tentatively interpreted that fast- and slow-decay donor components correspond to D2 and D3 donors as reported previously based on the similarity of dissociation temperatures.[10–12]

In conclusion, the HDs are the dominant donors in proton irradiation doping, even in m:Cz silicon samples, and the hydrogen-accelerated TDD model does not explain the experimental results effectively.

IV. DISCUSSION

In the present study, we found that (1) the HD concentration had no correlation with carbon and oxygen concentration, (2) the HD concentration clearly increased with the increase in irradiation dose, and (3) catalyzed TDD formation showed little effect on the observed donor concentrations even in m:Cz silicon with prolonged annealing. Based on these findings and the results from previous literatures, we hereby discuss the origin of HDs.

The incorporation of hydrogen in HDs has been demonstrated by the electronic absorption line-shift in deuterated silicon.[9,11,26] However, different interpretation approaches have been made regarding HD formation, which can be divided into two mechanisms: TDDs and point defects.

HD formation has been considered as an intermediate stage in the TDD formation process; this model states that HDs are partially hydrogen-passivated TDDs on the basis of similarity of the electron paramagnetic resonance spectra between the HD [labeled as NL10 (H)] and the singly ionized TDD (labeled as NL8).[26–28] Ulyashin *et al.*[39] reported that HD formation was suppressed in the denuded zone of hydrogenated *n*-type Cz wafers and suggested the role of oxygen in HD formation. Additionally, several studies have shown that TDD formation is equally enhanced by hydrogen and irradiation-induced defects via accelerated oxygen diffusion.[34–41] However, Simoen *et al.* revealed that the concentration of TDD$^{(+/++)}$, measured by DLTS, represents only a fraction (approximately 10%) of the created shallow donor concentration in hydrogenated *n*-type Cz silicon.[24] Additionally, other types of hydrogen-related shallow thermal donors (STDs) incorporating nitrogen or aluminum,

Published under an exclusive license by AIP Publishing

labeled as STD(NO) or STD(Al), respectively, were discovered in previous infrared absorption studies.[48,49]

In the present study, it was revealed that catalyzed TDD formation did not contribute to donor formation induced by proton irradiation. SIMS measurements revealed that nitrogen and aluminum concentrations were less than 1×10^{15} cm^{-3}, which ruled out nitrogen- or aluminum-incorporated STDs as representatives of observed donor concentrations. Therefore, it is reasonable to state that the formation processes of HDs and TDDs are independent of each other, and that HDs are the predominant donors in the proton irradiation doping process.

The fact that HDs can be formed in particle-irradiated silicon samples[9–23] indicates the incorporation of radiation-induced defects in the core of HDs. Several studies suggest that relevant radiation-induced core defects are VO[10,12] or C_iO_i complexes.[24,29,30] The former interpretation is based on the similarity of the annealing kinetics between VO complex and a type of HD (labeled as D1) observed by Hatakeyama and Suezawa in their infrared absorption study.[12] However, this model was ruled out because it was demonstrated that VOH is a deep acceptor with an electronic state at E_c −0.31 eV, and VOH_2 is electrically inert.[50–54] On the contrary, *ab initio* DFT calculations demonstrated that C_iO_iH rings and multi-(n) oxygen involved C_iO_nH complexes have shallow donor states.[29,30] However, the incorporation of carbon and oxygen in HDs has not been verified experimentally.

Our results ruled out the direct incorporation of carbon and oxygen in HDs. Therefore, the most plausible interpretation is that the core of the HD centers is formed by radiation-induced intrinsic defects. Additionally, the fact that HD formation in the irradiated silicon was inevitable when annealing at moderated temperature approximately at 250–550 °C suggests that the relevant intrinsic defects are vacancy clusters or interstitial silicon clusters rather than simple point defects.

Gorelkinskii *et al.*[19] suggested that interstitial-related defects participate in the HD formation process. Their electron paramagnetic resonance (EPR) results showed a large atomic reorientation energy (2.3 eV) of HDs, which was comparable to typical intrinsic-interstitial defect clusters such as tetra-interstitial silicon labeled as B3. Additionally, Tokmoldin and Mukashev[22] reported Si–H bond stretching modes originating from interstitial silicon clusters attached with hydrogen and associated these interstitial silicon-hydrogen complexes with HDs induced by proton irradiation. On the contrary, to the best of the authors' knowledge, vacancy cluster-related HDs have not been demonstrated experimentally nor theoretically. Therefore, the role of interstitial silicon and its clusters in the HD formation process is highly probable. Nevertheless, further investigation such as detailed EPR measurements is necessary to definitively correlate interstitial silicon clusters with the core of HD centers.

As regards the practical use of proton irradiation doping, the results obtained in the present study suggest that controlling the intrinsic defect formation, rather than the impurity concentration, is important in realizing the designed doping profiles. However, it should be noted that oxygen concentration indirectly affected the doping profiles because irradiation-induced oxygen-related defects preferentially trap diffusing hydrogen.[23] This trend suggests that the width of doping area depends on the oxygen the concentration of the silicon wafers.

V. CONCLUSIONS

n-type silicon wafers with different carbon and oxygen concentrations were irradiated with 2 MeV protons with doses varying from 1×10^{12} to 5×10^{14} cm^{-2} and subsequently annealed at 300–400 °C. Proton-irradiation induced HD concentration was estimated using the SR profiling technique. The HD concentration did not correlate with carbon concentration in the range of 5.6×10^{13}–2.0×10^{15} cm^{-3} and oxygen concentration in the range of less than 5×10^{15} to 1.8×10^{17} cm^{-3}. On the contrary, the HD concentration showed a strong increasing linear dependence with proton-irradiation dose at 350 and 400 °C and a square root dependence at 300 °C in the dose range of 1×10^{12} to 5×10^{14}. As regards annealing time dependence at 400 °C, fast- and slow-decay donor components were observed regardless of the type of wafer. Even in prolonged annealing for 137 h, donor concentrations were independent of oxygen concentrations in the silicon wafers. Based on these findings and the results from previous literatures regarding HD centers, we discussed the origin of HD centers. It is suggested that irradiation-induced intrinsic defects, presumably interstitial silicon clusters, represent the core of HD centers, and the incorporation of carbon- and oxygen-related defects, such as the TDDs and C_iO_nH, are ruled out in the HD formation process. The insights into the HD structure revealed in this study advances the understanding of the nature of HDs.

ACKNOWLEDGMENTS

The authors would like to thank J. Ito (SHI-ATEX Co., Ltd), S. Takemoto (Melco Semiconductor Engineering Corp.), and S. Samata (SUMCO Corp.) for their help with proton irradiation experiments, spreading resistance profiling measurements, and chemically activated DLTS measurements, respectively. The authors would also like to thank Y. Kamiura (Professor Emeritus of Okayama University) for helpful discussions and the critical review on this manuscript.

DATA AVAILABILITY

The data that support the findings of this study are available within the article.

REFERENCES

[1]F. Shimura, J. Appl. Phys. **59**, 3251 (1986).
[2]A. A. Kozlov and V. V. Kozlovski, Semiconductors **35**, 735 (2001).
[3]K. Takano, A. Kiyoi, and T. Minato, in *Proceedings of the 27th International Symposium Power Semiconductor Devices & ICs (ISPSD)*, Hong Kong, China (IEEE, 2015), Vol. 129.
[4]H. J. Schulze, H. Öfner, F.-J. Niedernostheide, J. G. Laven, H. P. Felsl, S. Voss, A. Schwagmann, M. Jelinek, N. Ganagona, A. Susiti, T. Wübben, W. Schustereder, A. Breymesser, M. Stadtmüller, A. Schulz, T. Kurz, and F. Lükermann, in *Proceedings of the 28th International Symposium on Power Semiconductor Devices & ICs (ISPSD)*, Prague, Czech Republic (IEEE, 2016), Vol. 355.
[5]M. Nemoto, T. Yoshimura, and H. Nakazawa, Appl. Phys. Express **1**, 051404 (2008).
[6]K. Nakmura, S. Nishizawa, and A. Furukawa, IEEE Trans. Electron Devices **67**, 2437 (2020).
[7]Y. Zohta, Y. Ohmura, and M. Kanazawa, Jpn. J. Appl. Phys. **10**, 532 (1971).

Published under an exclusive license by AIP Publishing

[8]Y. Gorelkinskii and N. N. Nevinnyi, Nucl. Instrum. Methods **209/210**, 677 (1983).
[9]J. Hartung and J. Weber, Phys. Rev. B **48**, 14161 (1993).
[10]V. P. Markevich, M. Suezawa, K. Sumino, and L. I. Murin, J. Appl. Phys. **76**, 7347 (1994).
[11]V. P. Markevich, M. Suezawa, and L. I. Murin, J. Appl. Phys. **84**, 1246 (1998).
[12]H. Hatakeyama and M. Suezawa, J. Appl. Phys. **82**, 4945 (1997).
[13]R. Job, F.-J. Niedernostheide, H.-J. Schulze, and H. Schulze, MRS Proc. **1108**, 1203 (2008).
[14]J. G. Laven, R. Job, W. Schustereder, H.-J. Schulze, F.-J. Niedernostheide, H. Schulze, and L. Frey, Solid State Phenom. **178/179**, 375 (2011).
[15]R. Job, J. G. Laven, F.-J. Nidernostheide, H.-J. Schulze, H. Schulze, and W. Schustereder, Phys. Status Solidi A **209**, 1940 (2012).
[16]J. G. Laven, R. Job, H.-J. Schulze, F.-J. Niedernostheide, W. Schustereder, and L. Frey, ECS J. Solid State Sci. Technol. **2**, P389 (2013).
[17]J. Hartung and J. Weber, J. Appl. Phys. **77**, 118 (1995).
[18]Y. Tokuda, A. Ito, and H. Ohshima, Semicond. Sci. Technol. **13**, 194 (1998).
[19]Y. V. Gorelkinskii, N. N. Nevinnyi, and K. A. Abdullin, J. Appl. Phys. **84**, 4847 (1998).
[20]E. Ntsoenzok, P. Desgardin, M. Saillard, J. Vernois, and J. F. Barbot, J. Appl. Phys. **79**, 8274 (1996).
[21]S. Z. Tokmoldin and B. N. Mukashev, Mater. Sci. Forum **258–263**, 223 (1997).
[22]S. Z. Tokmoldin and B. N. Mukashev, Phys. Status Solidi B **210**, 307 (1998).
[23]A. Kiyoi, N. Kawabata, K. Nakamura, and Y. Fujiwara, J. Appl. Phys. **129**, 025701 (2021).
[24]E. Simoen, Y. L. Huang, Y. Ma, J. Lauwaert, P. Clauws, J. M. Rafi, A. Ulyashin, and C. Claeys, J. Electrochem. Soc. **156**, H434 (2009).
[25]E. Simoen, C. Claeys, R. Job, A. G. Ulyashin, W. R. Fahrner, O. De Gryse, and P. Clauws, Appl. Phys. Lett. **81**, 1842 (2002).
[26]R. C. Newman, J. H. Tucker, N. G. Semaltianos, E. C. Lightowlers, T. Gregorkiewicz, I. S. Zevenbergen, and C. A. J. Ammerlaan, Phys. Rev. B **54**, R6803 (1996).
[27]S. A. McQuaid, R. C. Newman, and E. C. Lightowlers, Semicond. Sci. Technol. **9**, 1736 (1994).
[28]Y. V. Martynov, T. Gregorkiewicz, and C. A. J. Ammerlaan, Phys. Rev. Lett. **74**, 2030 (1995).
[29]J. Coutinho, R. Jones, P. R. Briddon, S. Öberg, L. I. Murin, V. P. Markevich, and J. L. Lindström, Phys. Rev. B **65**, 014109 (2002).
[30]C. P. Ewels, R. Jones, S. Öberg, J. Miro, and P. Deák, Phys. Rev. Lett. **77**, 865 (1996).
[31]W. Gotz, G. Pensl, and W. Zulehner, Phys. Rev. B **46**, 4312 (1992).
[32]Y. Kamiura, Y. Uno, and F. Hashimoto, Jpn. J. Appl. Phys. **32**, L1715 (1993).
[33]R. C. Newman, J. Phys.: Condens. Matter. **12**, R335–R365 (2000).
[34]H. J. Stein and S. K. Hahn, J. Appl. Phys. **75**, 3477 (1994).
[35]R. C. Newman, J. H. Tucker, A. R. Brown, and S. A. McQuaid, J. Appl. Phys. **70**, 3061 (1991).
[36]L. Tsetseris, S. Wang, and S. T. Pantelides, Appl. Phys. Lett. **88**, 051916 (2006).
[37]C. D. Lamp and D. J. James II, Appl. Phys. Lett. **62**, 2081 (1993).
[38]Y. L. Huang, Y. Ma, R. Job, W. R. Fahrner, E. Simoen, and C. Claeys, J. Appl. Phys. **98**, 033511 (2005).
[39]A. G. Ulyashin, R. Job, I. A. Khorunzhii, and W. R. Fahrner, Physica B **308–310**, 185 (2001).
[40]E. P. Neustroev, I. A. Antonova, V. P. Popov, V. F. Stas, V. A. Skuratov, and A. Y. Didyk, Nucl. Instrum. Methods Phys. Res. Sect. B **171**, 443 (2000).
[41]P. Hazdra and V. Komarnitskyy, Nucl. Instrum. Methods Phys. Res. Sect. B **253**, 187 (2006).
[42]K. Eriguchi, N. Mitsugi, and S. Samata, in *Proceedings of the 29th International Conference on Defects in Semiconductors (ICDS)*, Helsinki, Finland (ICDS, 2015).
[43]M. Yoneta, Y. Kamiura, and F. Hashimoto, J. Appl. Phys. **70**, 1295 (1991).
[44]J. F. Ziegler, J. P. Biersack, and U. Littmark, "The stopping and range of ions in solids," in *Stopping and Ranges of Ions in Matter* (Pergamon Press, New York, 1984), Vol. 1 of series.
[45]J. Coutinho, V. J. B. Torres, R. Jones, S. Öberg, and P. R. Briddon, J. Phys.: Condens. Matter **15**, S2809 (2003).
[46]S. J. Pearton, J. W. Corbett, and T. Shi, Appl. Phys. A **43**, 153 (1987).
[47]B. G. Svensson, C. Jagadish, A. Hallen, and J. Lalita, Phys. Rev. B **55**, 10498 (1997).
[48]R. E. Pritchard, M. J. Ashwin, J. H. Tucker, R. C. Newman, E. C. Lightowlers, T. Gregorkiewicz, I. S. Zevenbergen, C. A. J. Ammerlaan, R. Falster, and M. J. Binns, Semicond. Sci. Technol. **12**, 1404 (1997).
[49]R. C. Newman, M. J. Ashwin, R. E. Pritchard, and J. H. Tucker, Phys. Status Solidi B **210**, 519 (1998).
[50]R. C. Newman, J. Phys.: Condens. Matter **12**, R335 (2000).
[51]B. G. Svensson, A. Hallen, and B. U. R. Sundqvist, Mater. Sci. Eng. B **4**, 285 (1989).
[52]A. R. Peaker, J. H. Evans-Freeman, P. Y. Y. Kan, L. Rubaldo, I. D. Hawkins, K. D. Vernon-Parry, and L. Dobaczewski, Physica B **273/274**, 243 (1999).
[53]K. Bonde Nielsen, L. Dobaczewski, K. Goscinski, R. Bendesen, O. Andersen, and B. Bech Nielsen, Physica B **273/274**, 167 (1999).
[54]V. P. Markevich, L. I. Murin, M. Suezawa, J. L. Lindström, J. Countinho, R. Jones, P. R. Briddon, and S. Öberg, Phys. Rev. B **61**, 12964 (2000).

Published under an exclusive license by AIP Publishing